*Pioneer. Adv. Mater. 2026, 1(2): 1-8* *DOI: 10.48308/piadm.2025.241515.1009*

Shahid Beheshti University

**Pioneering Advances in Materials**

Journal homepage: http://piadm.sbu.ac.ir ISSN: 3115-7114

**Research paper**

# Investigation of the Magneto-Optic Faraday Rotation Effects in one Dimension of Plasma Photonic Crystal

***Leila Rajaei**, *Fatemeh Pourseyedaghaee***

***Department of Physics, Faculty of Basic Sciences, University of Qom, Qom, Iran***

**l-rajaei@qom.ac.ir*

**Article info:**

**Article history:**

Received: 13/09/2025

Accepted: 26/09/2025

**Keywords:** Photonic crystal, Magento-optic materials, Magneto-plasma photonic crystal, Bandgap.

**Abstract**

Magneto-plasma photonic crystals, composed of alternating layers of plasma and magneto-optical materials, offer dynamic control over the propagation of electromagnetic waves through tunable photonic bandgaps. The Faraday rotation has significant effect on these structures, where the interaction between circular birefringence induced by magnetic fields and the photonic band structure enhances the rotation of the polarization plane of transmitted light. This study investigates photonic crystal structures composed of layered media incorporating magneto-optical materials SiO2, TiO2, and yttrium iron garnet (YIG). The multilayer design, including air, dielectric, plasma, and magneto-optic layers, enables exploration of Faraday rotation and photonic bandgap modulation. Using transfer matrix method simulations, reflection and transmission coefficients were analyzed across a range of wavelengths, confirming photonic bandgap behavior consistent with theoretical expectations. Here we are shown that the enhanced Faraday rotation arises from circular birefringence induced by magnetic fields combined with the photonic band structure, increasing the effective light-matter interaction length. These findings highlight the importance of magneto-optical material selection and photonic crystal design in optimizing magneto-optical effects, facilitating the development of advanced photonic devices with tailored spectral characteristic.

## 1. Introduction

Photonic crystals are periodic optical nanostructures characterized by a refractive index that varies periodically in one, two or three dimensions. This periodicity influences the propagation of electromagnetic waves in a manner analogous to how atomic lattices affect electron movement in natural crystals [1,2]. One-dimensional photonic crystals consist of alternating dielectric or metal-dielectric layers, while two and three-dimensional photonic crystals have more complex periodic arrangements [3-5]. The fundamental operating principle of photonic crystals is the formation of photonic bandgaps—specific wavelength ranges in which light propagation is prohibited due to constructive interference and strong reflection [2,3]. These photonic bandgaps enable photonic crystals to function as optical filters, waveguides, amplifiers, beam splitters, and sensors [4-6]. Their sensitivity to external stimuli such as chemical composition, mechanical stress, electromagnetic fields, and temperature renders them highly versatile for various technological applications. When magnetic materials form part of the periodic structure, the resulting magnetophotonic crystals exhibit enhanced optical phenomena such as Faraday rotation and magneto-optical Kerr effects [7-9].

Plasma photonic crystals introduce further tunability by incorporating plasma layers with adjustable parameters. These layers allow dynamic modulation of photonic bandgaps under external magnetic fields, influencing the frequencies of light that can propagate through the structure. This magnetic control permits significant adjustment of the photonic band structure, enabling applications in plasma antennas, plasma lenses, and stealth technologies. Considerable theoretical and experimental research has addressed photonic crystals composed of metamaterials, superconductors, semiconductors, and plasma [10-13]. Notably, plasma photonic crystals respond quickly to changes in plasma parameters, affecting bandgap positions and transmission characteristics. Furthermore, magneto-optical effects in one-dimensional magnetophotonic crystals have been demonstrated to produce distinct phenomena such as Faraday band effects when light and magnetic fields interact perpendicularly.

Previous studies, including those by Nishizawa et al. (1997) [14], Sakai et al. (2005) [10], and more recent investigations, have documented bandgap modulation, energy flow changes under microwave irradiation, and the influence of magnetic fields in photonic crystal designs. These findings underscore the importance of material choice, structural design, and external stimuli in tailoring photonic crystal properties.

In this work, we focus on computational modeling of photonic crystals composed of plasma and dielectric layers, incorporating different magneto-optical materials to assess their effect on Faraday rotation and photonic bandgap formation. Given the high manufacturing costs of magnetophotonic crystals, accurate simulations enable efficient design and optimization to enhance device performance across optical and microwave regimes.

## 2. THEORETICAL MODEL AND NUMERICAL METHOD

Plasma-dielectric structure is |A|P|...|A|P|D|...|D|P|A|...|P|A| and we added different kind of magnetic layers (M) as silicon oxide $SiO_2$, titanium oxide $TiO_2$ and yttrium-iron garnet (YIG) $Y_3Fe_5O_{12}$ to have 3 magneto optic (MO) structure (|M|) as shown in figure1 to investigate effect of them on Faraday rotation. the crystal layers are parallel with the xy plane, as a periodicity of the structure is along the z-direction.

|A|: dielectric A
|D|: dielectric D
|P|: plasma
|M|: Magneto optic

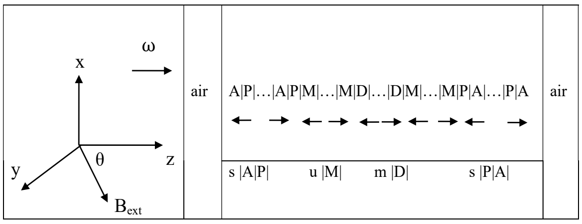


**Fig 1:** Schematic structure of the plasma photonic crystal.

In this paper, a 4 by 4 transfer matrix method is employed to study the magneto-optical effects in the target crystal under an external magnetic field. The wavelength ($\lambda_0$) is assumed to be 0.01 m. Dielectric layers (A) and (D) are $BaF_2$ and ZnSe respectively with refractive indices of $N_A$ = 1.4 and $N_D$ = 2.4. Thickness of plasma layer (P) is fixed to $\lambda_0/4$ and the thickness of dielectric layers is determined by $d_A = \lambda_0/4N_D$ and $d_D = \lambda_0/4N_A$. Permittivity tensor is:

$$\varepsilon_p = \begin{pmatrix} \varepsilon_{xx}(\omega) & \varepsilon_{xy}(\omega) & 0 \\ -\varepsilon_{yx}(\omega) & \varepsilon_{yy}(\omega) & 0 \\ 0 & 0 & \varepsilon_{zz}(\omega) \end{pmatrix} \quad (1)$$

$$\varepsilon_{xx}(\omega) = \varepsilon_{yy}(\omega) = \varepsilon_0 \left[1 - \frac{\omega_p(\omega - i\mathcal{V}_c)}{\omega[(\omega - i\mathcal{V}_c)^2 - \omega_c^2]}\right] \quad (2)$$

$$\varepsilon_{xy}(\omega) = \varepsilon_{yx}(\omega) = \frac{-i\varepsilon_0 \omega_p^2 \omega_c}{[(\omega - i\mathcal{V}_c)^2 - \omega_c^2]} \quad (3)$$

$$\varepsilon_{zz}(\omega) = \varepsilon_0 \left[1 - \frac{\omega_p^2}{\omega(\omega - i\mathcal{V}_c)}\right] \quad (4)$$

Where $\mathcal{V}_c$ represents the plasma collision frequency, $\omega_p = (e^2 n_e/\varepsilon_0 m_e)^{1/2}$ denotes the electron plasma frequency, $\omega_c = (eB/m_e)$ denotes plasma syclotron frequency with B being magnetic field, $\varepsilon_0$ represents dielectric constant, e is electron charge, $n_e$ reresents plasma density and $m_e$ electron mass. generalized permittivity tensor is given by following [Feng Zhang 2012]:
In order to investigate the impact of the declination angle of the magnetic field, it is imperative to incorporate an adapted permittivity tensor to accommodate the alterations in the orientation of the magnetic field. By adhering to the methodology delineated in [30], the generalized plasma permittivity of tensor can be expressed as:

$$\varepsilon_{gp} = \mathrm{R}\varepsilon_p R^{-1} \quad (5)$$

where

$$\begin{cases} \mathrm{R} = \begin{pmatrix} 0 & 1 & 0 \\ -\cos(\theta) & 0 & \sin(\theta) \\ \sin(\theta) & 0 & \cos(\theta) \end{pmatrix} \\ R^{-1} = \begin{pmatrix} 0 & -\cos(\theta) & \sin(\theta) \\ 1 & 0 & 0 \\ 0 & \sin(\theta) & \cos(\theta) \end{pmatrix} \end{cases} \quad (6)$$

And $\theta$ is declination angle of the magnetic field. Generalized permittivity of dielectric has this form:

$$\varepsilon_{gDi} = \varepsilon_{Di} = \begin{pmatrix} \varepsilon_d & 0 & 0 \\ 0 & \varepsilon_d & 0 \\ 0 & 0 & \varepsilon_d \end{pmatrix} \quad (8)$$

The waves are assumed to be circularly polarized.

$$\begin{aligned} E^{(j)} = \frac{1}{\sqrt{2}} \{ & E_{01}^{(j)}(\hat{X} + i\hat{Y}) \exp\left[-i\frac{\omega}{c} N_+^{(j)}(z - z_j)\right] \\ & + E_{02}^{(j)}(\hat{X} + i\hat{Y}) \exp\left[i\frac{\omega}{c} N_+^{(j)}(z - z_j)\right] \\ & + E_{03}^{(j)}(\hat{X} + i\hat{Y}) \exp\left[-i\frac{\omega}{c} N_-^{(j)}(z - z_j)\right] \\ & + E_{04}^{(j)}(\hat{X} + i\hat{Y}) \exp\left[i\frac{\omega}{c} N_-^{(j)}(z - z_j)\right] \} \end{aligned} \quad (9)$$

where

$$N_{(j)}^2 = 1 - \frac{\left(\frac{\omega_p}{\omega}\right)^2}{\left[1 + i\frac{v_c}{\omega} - \frac{\left(\frac{\omega_c}{\omega}\sin(\theta)\right)^2}{2\left(1 + i\frac{v_c}{\omega} - \frac{\omega_p^2}{\omega^2}\right)}\right] \pm \sqrt{\frac{\left(\frac{\omega_c}{\omega}\sin(\theta)\right)^4}{4\left(1 + i\frac{v_c}{\omega} - \frac{\omega_p^2}{\omega^2}\right)} + \left(\frac{\omega_c}{\omega}\cos(\theta)\right)^2}} \quad (10)$$

$$N_{(j)}^2 = \varepsilon_{Di} \quad (11)$$

The wave transmission through each layer is expressed using the transfer matrix as follows:

$$D^{(j-1)} E_0^{(j-1)} = D^{(j)} P^{(j)} E_0^{(j)} \quad (12)$$

where

$$D^{(j)} = \begin{bmatrix} 1 & 1 & 0 & 0 \\ N_+^{(j)} & N_+^{(j)} & 0 & 0 \\ 0 & 0 & 1 & 1 \\ 0 & 0 & N_-^{(j)} & N_-^{(j)} \end{bmatrix} \quad (13)$$

$$P_j = \begin{bmatrix} \exp(+i\beta_+^{(j)}) & 0 & 0 & 0 \\ 0 & \exp(-i\beta_+^{(j)}) & 0 & 0 \\ 0 & 0 & \exp(+i\beta_-^{(j)}) & 0 \\ 0 & 0 & 0 & \exp(-i\beta_-^{(j)}) \end{bmatrix} \quad (14)$$

The relationship between the incident wave and the transmitted wave across all layers of the photonic crystal, based on the transmission matrix, is expressed as follows:

$$\begin{bmatrix} E_+^i \\ E_+^r \\ E_-^i \\ E_-^r \end{bmatrix} = \begin{bmatrix} M_{11} & M_{12} & 0 & 0 \\ M_{21} & M_{22} & 0 & 0 \\ 0 & 0 & M_{33} & M_{34} \\ 0 & 0 & M_{43} & M_{44} \end{bmatrix} \begin{bmatrix} E_+^I \\ 0 \\ E_-^t \\ 0 \end{bmatrix} \quad (15)$$

Here $E_{\pm}$ a positive sign denotes a right-handed circularly polarized wave, while a negative sign denotes a left-handed circularly polarized wave. $M$ is defined as:

$$M = [D^0]^{-1}\left(\prod_{j=1}^{J} G^{(j)}\right)D^{(J+1)} \tag{16}$$

$$G^{(j)} = \begin{bmatrix} \cos\beta_+^{(j)} & \frac{i}{N_+^{(l)}}\sin\beta_+^{(j)} & 0 & 0 \\ iN_+^{(j)}\sin\beta_+^{(l)} & \cos\beta_+^{(j)} & 0 & 0 \\ 0 & 0 & \cos\beta_-^{(j)} & \frac{i}{N_-^{(l)}}\sin\beta_-^{(j)} \\ 0 & 0 & iN_-^{(j)}\sin\beta_-^{(j)} & \cos\beta_-^{(j)} \end{bmatrix}$$

Where:

$$t_+ = (M_{11})^{-1},\quad t_- = (M_{33})^{-1},\quad r_+ = (M_{21})/(M_{11}),\quad r_- = (M_{43})/(M_{33}). \tag{17}$$

The total transmission and reflection are written as:

$$T = \frac{1}{2}(|t_+^2| + |t_-^2|) \tag{18}$$

$$R = \frac{1}{2}(|t_+^2| + |r_-^2|) \tag{19}$$

It is well known that the Faraday effect causes a polarization rotation which is proportional to the projection of the magnetic field along the direction of the light propagation. Therefore, we can assume the angle of faraday rotation is written in this form:

$$\theta_f = \frac{1}{2}\arg(\xi_f) \tag{20}$$

where $\xi_f = \frac{M_{33}}{M_{11}}$.

For magneto optic layer, we add |M| layers and by following approach presented in [dadonevoka and zhang] will have:

$$\varepsilon_M = \begin{pmatrix} \varepsilon^{(M)} & 0 & 0 \\ 0 & \varepsilon^{(M)} & i\varepsilon' \\ 0 & -i\varepsilon' & \varepsilon^{(M)} \end{pmatrix} \tag{21}$$

Where the off-diagonal material tensor elements are: $\varepsilon' = 2.47 \times 10^{-4}$

$$\varepsilon'_M = T\varepsilon_M T^{-1} \tag{22}$$

$$\varepsilon'_M = \begin{pmatrix} \varepsilon^{(M)} & i\varepsilon'\sin(\theta) & i\varepsilon'\cos(\theta) \\ -i\varepsilon'\sin(\theta) & \varepsilon^{(M)} & 0 \\ -i\varepsilon'\cos(\theta) & 0 & \varepsilon^{(M)} \end{pmatrix} \tag{23}$$

And finally, $N$ for our problem is written in this form:

$$N^2 = \frac{2\varepsilon^{2M} - \varepsilon'^2\cos^2\theta}{2\varepsilon^M} \pm \frac{\sqrt{\left(2\varepsilon^{2M} - \varepsilon'^2\cos^2\theta\right)^2 - 4\,\varepsilon^M(\varepsilon^{3M} - \varepsilon^M\varepsilon')}}{2\varepsilon^M} \tag{24}$$

where

$$\varepsilon^{(M)}(\lambda) = f_0^{(M)} + \sum_{i=1}^{3}\frac{f_i^{(M)}\lambda^2}{\lambda^2 - \left(\lambda_i^{(M)}\right)^2}$$

$$\mathrm{M} = \mathrm{A, B, C} \tag{25}$$

Where Sellmeier coefficients $f_i^{(M)}$ and $\lambda_i^{(M)}$are gathered in Table1.

| Material | sellmeier coefficients |
|---|---|
| $TiO_2$ | $f_0^{(A)} = 5.913$ , $f_1^{(A)} = 0.2441$ , $f_2^{(A)} = 0$ , $f_3^{(A)} = 0$, $\lambda_1^{(A)} = 0.0803\ \mu m$ , $\lambda_2^{(A)} = 0$ , $\lambda_3^{(A)} = 0$. |
| $SiO_2$ | $f_0^{(B)} = 1$ , $f_1^{(B)} = 0.6961663$ , $f_2^{(B)} = 0.4079426$ , $f_3^{(B)} = 08974794$, $\lambda_1^{(B)} = 0.0684043\ \mu m$ , $\lambda_2^{(B)} = 0.1162414\ \mu m$ , $\lambda_3^{(B)} = 9.896162\ \mu m$. |
| $Y_3Fe_5O_{12}$ | $f_0^{(c)} = 1$ , $f_1^{(c)} = 3.739$ , $f_2^{(c)} = 0.79$ , $f_3^{(c)} = 0$, $\lambda_1^{(c)} = 0.028\ \mu m$ , $\lambda_2^{(c)} = 10.00\ \mu m$ , $\lambda_3^{(c)} = 0$. |

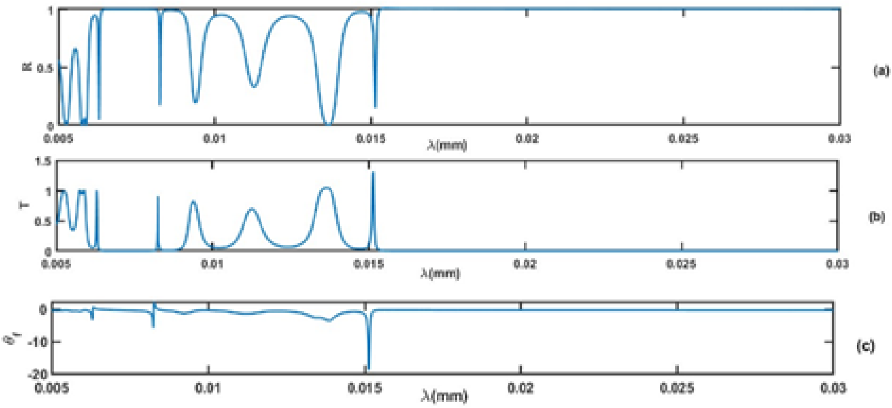


**Fig 2:** The reflection, transmission and Faraday rotation from photonic crystal with magneto optic SiO2 a) the reflection, b) transmission, c) Faraday rotation.

**3. Numerical results and discussion**

In this study, we examine two models of photonic crystals comprising two magneto-optic materials. It is important to emphasize that the photonic crystal structure is composed of layered media arranged in the sequence: air, dielectric, plasma, and magneto-optic materials.

In fact, in this section, we compared the Faraday rotation of 3 magneto-optic materials (SiO2, TiO2 and YIG materials) with the plasma-dielectric structure.

|A|P|...|A|P|M|...|M|D|...|D|M|...|M|P|A|...|P|A|,
s=m=u=4

|M|: magnetic layer as SiO2, TiO2 and YIG
s: number of |A|P| and number of |P|A|.
m: number of |D|
u: number of |M|
p: number of |A|P|M| and number of |M|P|A|

Initially, the magneto-optic material '$Sio_2$' is integrated into the photonic crystal structure. Subsequently, the magnitude of the Faraday rotation effect is quantitatively analyzed, alongside a comprehensive examination of the transmission and reflection coefficients to evaluate the optical behavior of the system, the parameters of used in this section as follows:

$f_0 = 1,\ f_1 = 0{,}6961663,\ f_2 = 0{,}4079426$
$f_3 = 0{,}8974794,\ l_1 = 0{,}8974794 * 10^{-6}$ ,
$l_2 = 0{,}1162414 * 10^{-6}$ , $l_3 = 9{,}896162 * 10^{-6}$

In Figures 2a and 2b, the reflection and transmission coefficients of electromagnetic wave from photonic crystal were analyzed by incident electromagnetic waves with varying wavelengths (measured in millimeter, mm). According to these plots, for $0.0063 < \lambda < 0.00824$ is the first photonic bandgap region. And the second region of photonic bandgap is $0.01512 < \lambda$, the structure shows complete reflection, thus behaving as an opaque medium in this spectral range. This behavior confirms the photonic bandgap properties of the crystal, consistent with theoretical predictions for such multilayer magneto-optic structures.
In Fig 2c, the Faraday rotation is examined as a function of the wavelength. The data reveal that Faraday rotation is negligible across most wavelengths; however, pronounced rotation occurs at wavelengths of 0.01512 mm, 0.00824mm, 0.0063mm. These findings indicate that at these particular wavelengths, the electromagnetic wave undergoes total transmission. Notably, Faraday rotation manifests in the transmitted component, consistent with the magneto-optic effect, where the polarization plane of light is rotated due to the presence of a magnetic field within the

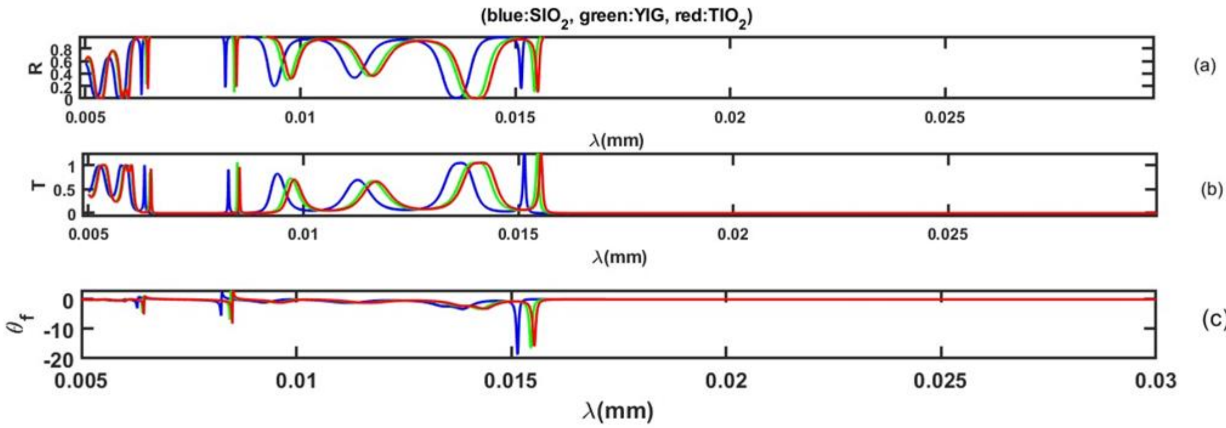


**Fig 3:** The reflection, transmission and Faraday rotation from photonic crystal with magneto optic for three magneto optic materials. a) the reflection, b) transmission, c) Faraday rotation.

magneto-optic layers of the photonic crystal. Such enhanced Faraday rotation near photonic band edges and defect modes has been theoretically and experimentally demonstrated in one-dimensional multilayer magneto-photonic systems, where the localization of light leads to increased magneto-optical interaction [15]. The use of magnetic defect layers to enhance Faraday rotation has also been reported, confirming the strong coupling between light and the magneto-optic medium [16].

To investigate the effects of different magneto-optical materials on the photonic crystal structure, we analyze configurations incorporating the magneto-optical materials Titanium Dioxide $TIO_2$, $SIO_2$ and Yttrium iron garnet YIG. These materials are selected due to their distinct magneto-optical properties, which are expected to influence key optical phenomena such as Faraday rotation and photonic bandgap modulation.

By comparing the results obtained with each material, we aim to elucidate how variations in magneto-optical response impact the transmission, reflection, and polarization characteristics of the photonic crystal. The outcomes of these analyses are presented in Figure 2.

It should be mentioned that the parameters of used for YIG as follows:

$f_0 = 1, f_1 = 3.739, f_2 = 0.79, f_3 = 0,$
$l_1 = 0.28 * 10^{-6}, l_2 = 10 * 10^{-6}, l_3 = 0,$
x=1543

and for $TiO_2$ as follows:

$f_0 = 5.913, f_1 = 0.244, f_2 = 0, f_3 = 0,$
$l_1 = 0.0803 * 10^{-6}, l_2 = 0, l_3 = 0,$
$x = 0.01552$

To investigate the effects of different magneto-optical materials on the photonic crystal structure, we analyze configurations incorporating the magneto-optical materials $SIO_2$, $TIO_2$ and yttrium aluminum garnet YIG. These materials are selected due to their distinctive magneto-optical parameters, including their permittivity, refractive indices, and absorption coefficients, which directly influence Faraday rotation and photonic bandgap modulation. Quantitative analysis reveals that the photonic bandgap shifts in response to changes in the magneto-optical material properties, with the bandgap for YIG initiating at a longer wavelength compared to $TiO_2$ and $SIO_2$. The magnitude of the bandgap shift is on the order of a few nanometers, reflecting subtle but significant tuning of the photonic crystal structure. These findings are consistent with transfer matrix method simulations that account for complex dielectric tensors including non-diagonal components responsible for gyrotropic magneto-optical effects. The results illustrated in Figures 3a and 3b demonstrate that while the overall bandgap width remains nearly constant,

the spectral position can be finely tuned by selecting appropriate magneto-optical constituents, enabling tailored photonic devices with optimized magneto-optic performance.
Faraday rotation in magneto-optical photonic crystals arises from the interplay between the magnetic field-induced circular birefringence in the magneto-optical material and the photonic band structure of the crystal. When linearly polarized light propagates through such a medium, the difference in refractive indices for left- and right-circularly polarized components causes the polarization plane to rotate.
This effect is strongly wavelength-dependent and is significantly enhanced near the edges of the photonic bandgap, where the density of optical states is high and light experiences multiple Bragg reflections within the structure. The constructive interference at these wavelengths leads to longer effective interaction lengths and increased Faraday rotation angles compared to bulk materials [17]. The maximum rotation typically occurs at wavelengths near the bandgap edge, as seen in Fig 3c, where the rotation peak around 0.001512 coincides with the bandgap onset. Moreover, the magneto-optical response is influenced by complex dielectric tensors reflecting gyrotropic properties, which depend on the applied magnetic field and material parameters, and can be modeled by transfer matrix methods or coupled mode theory [18].

## 4. Conclusion

This study investigates photonic crystal structures composed of layered media incorporating magneto-optical materials, specifically SiO2, TiO2, and yttrium iron garnet (YIG). The arrangement of air, dielectric, plasma, and magneto-optic layers creates a versatile platform for exploring magneto-optical phenomena such as Faraday rotation and photonic bandgap modulation. Using transfer matrix method simulations, the reflection and transmission coefficients were analyzed over a range of wavelengths, revealing the characteristic photonic bandgap behavior consistent with theoretical predictions for multilayer magneto-optic systems.
Faraday rotation was found to be negligible at most wavelengths but showed pronounced peaks near the photonic band edges and defect modes, particularly where total transmission occurs. These enhancements arise from the strong light confinement and multiple scattering within the photonic crystal, intensifying the magneto-optical coupling. Quantitative comparisons among the three magneto-optic materials demonstrate material-dependent shifts in the photonic bandgap, with YIG exhibiting a bandgap onset at longer wavelengths compared to TiO2 and SiO2. While the magnitude of this spectral shift is modest, it provides a means to finely tune optical properties by selecting appropriate magneto-optical constituents.
Theoretical analysis confirms that Faraday rotation enhancement in these structures results from the combined effects of circular birefringence induced by the magnetic field and the photonic band structure, which increases the effective interaction length of light within the magneto-optical media. This tunability and enhanced magneto-optical response provide significant opportunities for designing advanced photonic devices, including optical isolators, modulators, and sensors with tailored spectral characteristics.
Overall, the study highlights the critical role of magneto-optical material selection and photonic crystal design in optimizing Faraday rotation and photonic bandgap features, advancing the development of functional magnetophotonic devices.

## References


1. *Yablonovitch, E; Gmitter, T; Leung, K (1991). "Photonic band structure: The face-centered-cubic case employing nonspherical atoms". Physical Review Letters.* ***67*** *(17): 2295–2298. Bibcode:1991PhRvL..67.2295Y. doi:10.1103/PhysRevLett.67.2295.*
2. *Haus, J. W. (Ed.). (2016). Fundamentals and applications of nanophotonics. Woodhead Publishing.*
3. *Ustyantsev, M. (2007). Desing and Analysis of Metallo-Dielectric Photonic Crystalls. Universitat Rovira i Virgili.*

4. *Krauss, T. F., & Richard, M. D. L. R. (1999). Photonic crystals in the optical regime—past, present and future. Progress in Quantum electronics, 23(2), 51-96.*
5. *Yablonovitch, E. J. J. B. (1993). Photonic band-gap structures. Journal of the optical society of America B, 10(2), 283-295.*
6. *Lonergan, A., & O'Dwyer, C. (2023). Many facets of photonic crystals: From optics and sensors to energy storage and photocatalysis. Advanced Materials Technologies, 8(6), 2201410.*
7. *Subkhangulov, R. R., Mikhaylovskiy, R. V., Zvezdin, A. K., Kruglyak, V. V., Rasing, T., & Kimel, A. V. (2016). Terahertz modulation of the Faraday rotation by laser pulses via the optical Kerr effect. Nature Photonics, 10(2), 111-114.*
8. *Argyres, P. N. (1955). Theory of the Faraday and Kerr effects in ferromagnetics. Physical Review, 97(2), 334.*
9. *Shinagawa, K. (2000). Faraday and Kerr effects in ferromagnets. In Magneto-optics (pp. 137-177). Berlin, Heidelberg: Springer Berlin Heidelberg.*
10. *Sakai, K. L. (2005). Language acquisition and brain development. Science, 310(5749), 815-819.*
11. *Khanikaev, A. B., Baryshev, A. V., Inoue, M., Granovsky, A. B., & Vinogradov, A. P. (2005). Two-dimensional magnetophotonic crystal: Exactly solvable model. Physical Review B—Condensed Matter and Materials Physics, 72(3), 035123.*
12. *Assad, M. A., & Elbahri, M. (2025). Perfect ultraviolet absorbers via disordered polarizonic metasurfaces for multiband camouflage and stealth technologies. Advanced Functional Materials, 35(14), 2418271.*
13. *Ali, A., Mitra, A., & Aïssa, B. (2022). Metamaterials and metasurfaces: A review from the perspectives of materials, mechanisms and advanced metadevices. Nanomaterials, 12(6), 1027.*
14. *Nishizawa, T., Okamoto, H., Konishi, K., Yoshizawa, H., Miyakawa, Y., & Mayumi, M. (1997). A novel DNA virus (TTV) associated with elevated transaminase levels in posttransfusion hepatitis of unknown etiology. Biochemical and biophysical research communications, 241(1), 92-97.*
15. *Dadoenkova, N. N., Dadoenkova, Y. S., Panyaev, I. S., Sannikov, D. G., & Lyubchanskii, I. L. (2018). One-dimensional dielectric bi-periodic photonic structures based on ternary photonic crystals. Journal of Applied Physics, 123(4).*
16. *Malekshahi, S., Khalajmasoumi, M., Mohammad-Doost, H., Sojdehee, M., & Aboutorab, S. (2023). Study of Alterations, fluid inclusions and sulfur and oxygen isotope compositions in Sarkuh porphyry copper deposit, Kerman. Scientific Quarterly Journal of Geosciences, 33(3), 159-182.*
17. *Koerdt, C., Rikken, G. L. J. A., & Petrov, E. P. (2003). Faraday effect of photonic crystals. Applied Physics Letters, 82(10), 1538-1540.*
18. *Dadoenkova, Y. S., Dadoenkova, N. N., Lyubchanskii, I. L., Kłos, J. W., & Krawczyk, M. (2017). Faraday effect in bi-periodic photonic-magnonic crystals. IEEE Transactions on Magnetics, 53(11), 1-5.*